Composites Communications 33 (2022) 101239

Contents lists available at ScienceDirect

Composites Communications

journal homepage: www.elsevier.com/locate/coco

3D printing of continuous carbon fibre reinforced powder-based epoxy composites

Haoqi Zhang [1], Ka Zhang [1], Aonan Li [1], Lei Wan [1], Colin Robert, Conchúr M. Ó Brádaigh, Dongmin Yang [*]

School of Engineering, Institute for Materials and Processes, University of Edinburgh, EH9 3FB, Edinburgh, UK

ARTICLE INFO

Keywords:
3D printing
Filament fabrication
Continuous carbon fibre reinforced composites
Powder epoxy
Electrostatic powder deposition

ABSTRACT

This paper presents an experimental study on 3D printing of continuous carbon fibre reinforced thermoset epoxy composites. Powder-based solid epoxy was electrostatically flocked on the 1K continuous carbon fibre tow and then melted to fabricate composite filaments. The produced filament was printed using a modified extrusion-based printer which melted and deposited the filament following designed printing paths, to form multilayer preforms with complex geometries. After vacuum bagging and oven curing, high tensile strength (1372.4 MPa) and modulus (98.2 GPa) were obtained in the fibre direction due to the good wettability of epoxy and the consequent high fibre volume fraction (56%). The tensile tests of open-hole composites were also conducted, in which the sample with designed stress-lines fibre paths was seen to improve the ultimate strength by 95% compared with the mechanically-drilled sample. Other case studies, such as a spanner and a lattice structure, further demonstrated the design freedom of produced filaments for complex geometries.

1. Introduction

3D printing of composites has attracted significant attention in the past few years, thanks to advantages including flexible design, rapid prototyping and waste reduction [1,2]. The reinforcements, ranging from 100 μm length discontinuous fibres to continuous fibres [3,4], can be introduced in the 3D printing technologies to enhance the mechanical and thermal performance of the finished parts [5]. The polymer system of 3D-printed composites could be thermoplastic or thermoset, for example, discontinuous fibres have been impregnated with a thermoplastic matrix and printed out using fused filament fabrication (FFF) [6], or mixed with a low viscosity thermoset resin and printed out through the direct-ink writing (DIW) process [7–9]. Additive manufacturing of continuous fibre reinforced composites has been found to be more challenging in terms of filament fabrication as well as printing process control [10–12]. Despite these problems, continuous fibres are generally preferred as they offer superior mechanical performance and more design freedom, such as the customisation of fibre orientation [13,14]. Most of the reported studies in the literature used thermoplastic as the matrix for the material-extrusion technique, for instance, polyamides (PA) [15–17], polylactic acid (PLA) [18–20] and polyether ether ketone (PEEK) [21,22]. One of the challenging issues of using a thermoplastic matrix is its high viscosity, which could lead to substantial air voids within and in-between the printing beads [11,23]. High fibre volume fractions are also difficult to achieve due to insufficient impregnation in the filament. These factors all reduce the stiffness and strength as compared to the conventionally manufactured composites. In addition, the thermoplastic filament with continuous fibres is quite expensive due to the infrastructure cost of the high-temperature and high-pressure pultrusion technique, especially for those with 1K continuous carbon fibre (CCF) tow [24].

Attempts have been made to address these issues. For example, in-situ ultrasonic treatment was used to modify the interface corresponding to the wettability of fibre and PLA [20]. Also, a similar roller compression technique used for automated fibre placement (AFP) has been adopted to reduce the void content of 3D-printed CCF/PA composites [25]. However, the fibre volume fraction was still lower than 35% when using the thermoplastic matrix. On the other hand, thermoset polymers have also been adopted in 3D printing of continuous carbon fibres. The main advantage of using thermosetting polymers are their low viscosity and generally good wettability and interfacial bonding with carbon fibres. Callens et al. simultaneously fed two polymer

* Corresponding author.
E-mail address: Dongmin.Yang@ed.ac.uk (D. Yang).
[1] These authors contribute equally.

https://doi.org/10.1016/j.coco.2022.101239
Received 12 April 2022; Received in revised form 23 June 2022; Accepted 28 June 2022
Available online 30 June 2022

matrices (thermoset and thermoplastic) with continuous fibre to achieve a 40% fibre volume fraction [26]. The UV curable resin was also adopted to enable in-situ (or immediately) curing in the process [27], however, this in-nozzle impregnation technique with liquefied thermoset resin resulted in a low fibre fraction (only 8.6%) and printing inaccuracy [28]. Another study used a heated tank to melt the solid epoxy and the 3K continuous carbon fibres were impregnated when passing through the bath [29]. The fabricated filament was then printed using the extrusion-based technique, followed by oven curing. The large volumes of melted epoxy, curing agent, catalyst and other additives may experience evaporation over long times, leading to health and safety risks from Volatile Organic Compounds (VOCs). Unlike the liquid impregnation which is delivered via an evaporating solvent, powdered polymers produce little or no VOCs and do not result in waste disposal problems [30], thus they have been widely used in the coating industry [31,32]. The powders are applied to parts via electrostatic spray or other deposition processes [33]. Once applied, the powder is heated to form a molten polymer coat and, at a sufficiently high temperature, the latent curing agents activate and the coating cures [34].

In this study, a powder-based epoxy is coated on the 1K continuous carbon fibre tow through an in-house developed electrostatic powder deposition tapeline. The coated epoxy powders are heated by infrared lighting and cooled rapidly, thus minimising any possible evaporation of VOCs. The low-cost fabricated filament is then printed on a modified extrusion-based printer to manufacture unidirectional lamina and open-hole composite preforms with designed curved fibre paths, followed by vacuum bagging and oven curing.

2. Low-cost CCF/epoxy filament

2.1. Materials introduction

The thermoset epoxy (PE6405, density 1.22 g/cm3) was engineered by Swiss CMT (Siebnen, Switzerland) and produced by FreiLacke

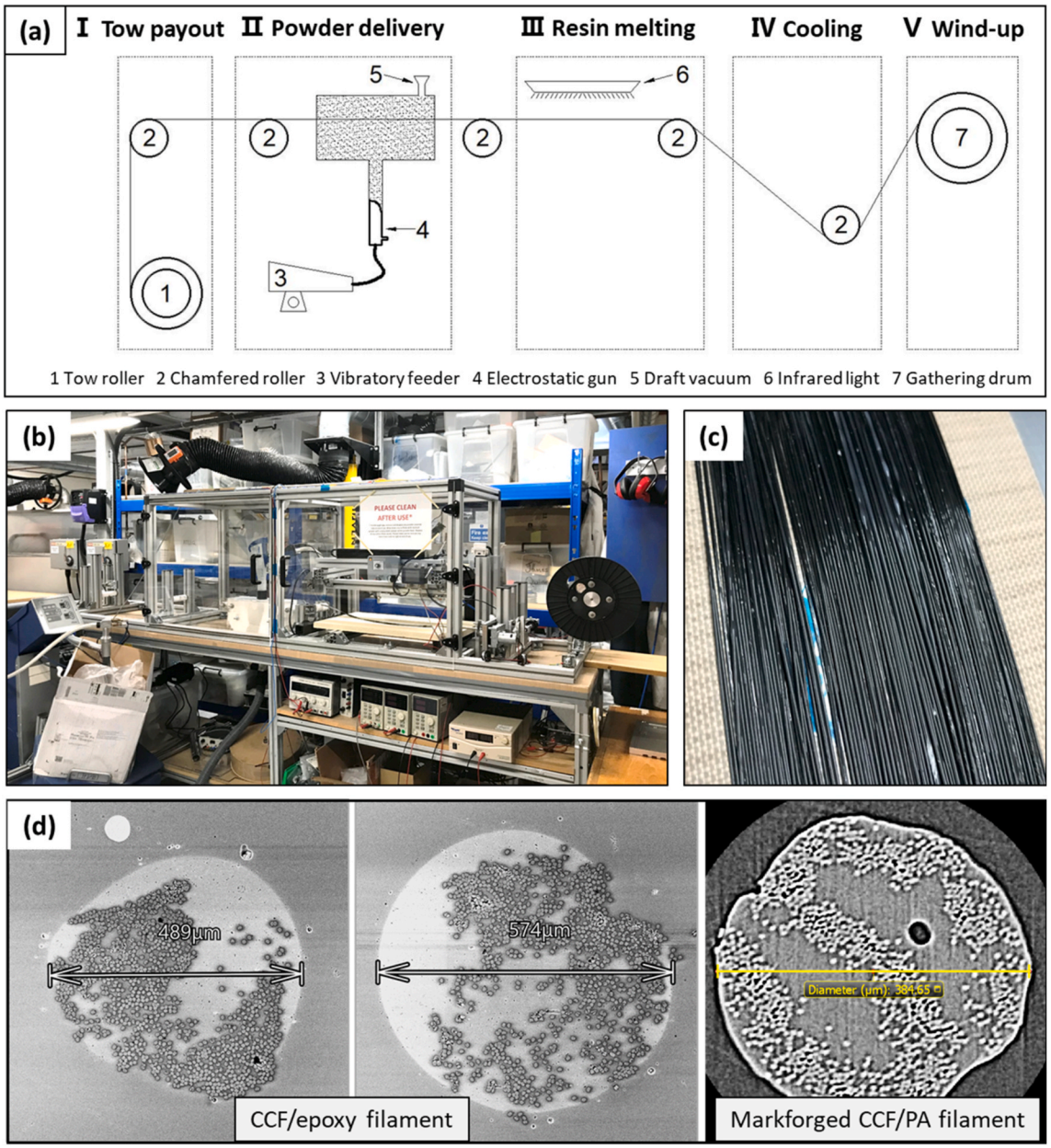

Fig. 1. (a) Schematic of the tapeline design (b) the setup of the powder-based tapeline (c) produced 1K filament on the gathering drum (d) cross-section of CCF/epoxy and CCF/PA filaments [12].

(Bräunlingen, Germany), in which latent curing agents were mixed in the powders to store the epoxy in a glassy state at ambient conditions [34]. The solid epoxy is produced from a proprietary formulation through extrusion, followed by grinding into powders with a particle diameter in the 10–50 μm range. The powder status allows for easy transportation and storage of the resin and enables the fibres to be coated through an electrostatic deposition process. The solid powder-based epoxy melts at around 45–60 °C, with a minimal viscosity of 1.26 Pa s. The curing agent requires a temperature of at least 150 °C for reaction initiation [35,36]. The low melt viscosity and the low rate of cure below 120 °C allow a good wettability with 1K T300 carbon fibre tow (sourced from Toray®) during the fabrication of continuous filaments [37].

2.2. Fabrication tapeline of low-cost 1K CCF/epoxy filament

In this study, a powder-based tapeline [37] was used to produce environmentally-friendly 1K continuous carbon fibre filaments for 3D printing. The schematic of the tapeline design and its setup can be found in Fig. 1a. In Step I, the fibres are drawn from the tow roller, guided using chamfered PTFE rollers and tensioned with the tow roller and gathering drum. In Step II, the fibres are pulled through the deposition chamber where an electrostatic gun (Encore® spray gun with 90 kV at 60 μA) spray deposits charged powder particles supplied by a vibratory feeder onto the fibres vertically. It is noted that the amount of epoxy coated on the filament would be decreased as the airflow of vibratory feeder is weakened and the power of electrostatic gun is lowered. A draft vacuum is utilised to collect redundant powder which is not attracted by the fibres. After deposition, in step III, heat is applied to the coated fibres via an infrared light in order to melt the powder. The chamber temperature was set to reach 120 °C. The fibre tape is then cooled and solidified within 4 s in ambient air under tension between two rollers in step Ⅳ. A circular-similar cross-section with a diameter of about 0.5–0.6 mm is obtained for the 1K filament, with an average fibre fraction of 23%. Finally, the impregnated tape is wound-up on the gathering drum (in Fig. 1c), which is motorised to keep the whole line under tension in the step Ⅴ. This tensile force also influences the spread-out of the fibre tow on the rollers and subsequently more epoxy powders are coated on filaments with wider spread-out. As shown in Fig. 1d, good wettability between fibre and matrix can be seen and no apparent voids were found to be trapped between the fibres, unlike the 1K CCF/thermoplastic filaments from Markforged® [12].

2.3. 3D printing and oven curing

A Prusa i3 printer (Fig. 2 a & b) was used with a filleted brass nozzle

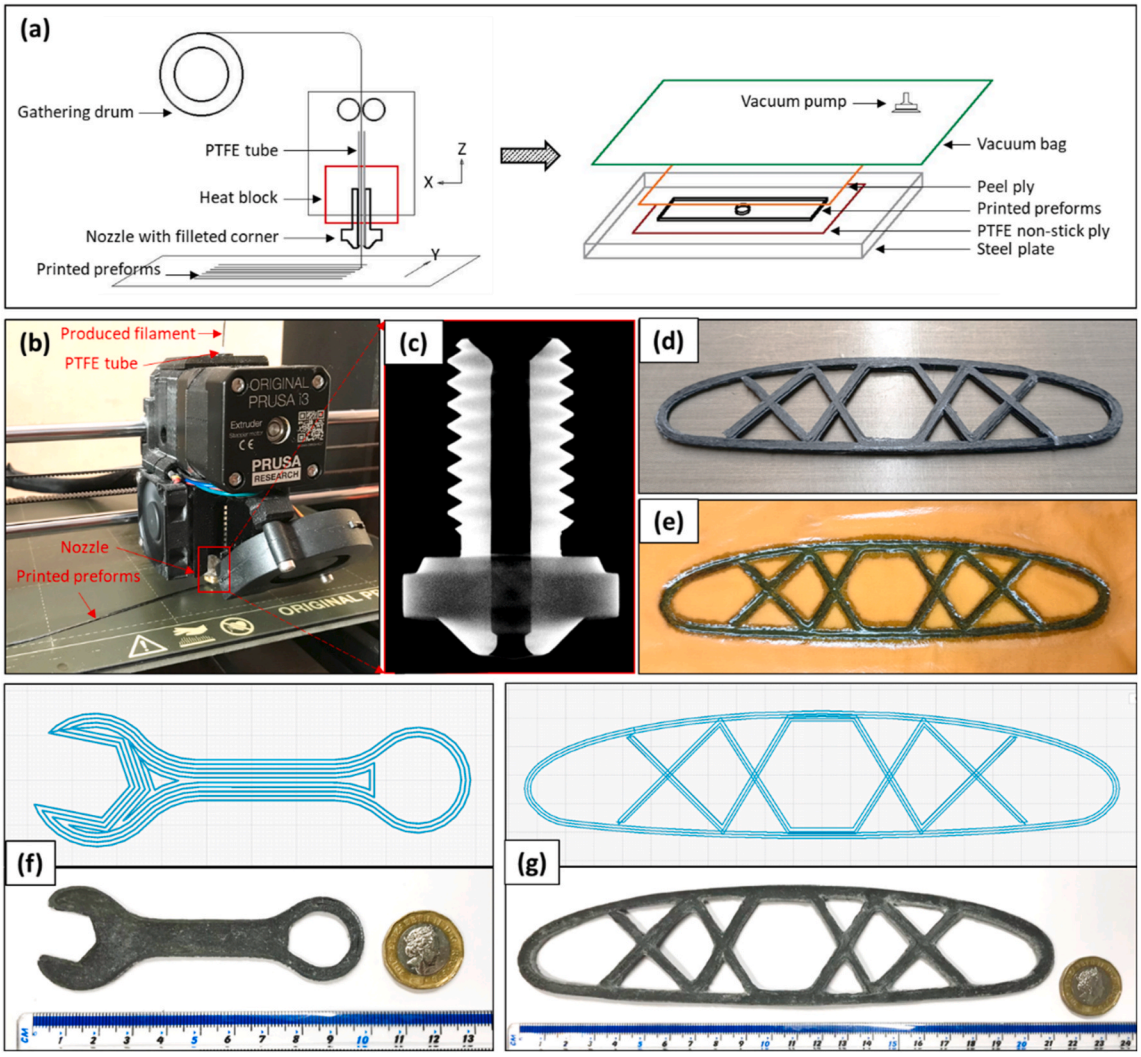

Figure 2. (a) Schematic of the printing and curing processes (b) modified Prusa i3 print-head for CCF/epoxy filament printing (c) brass nozzle for continuous filament printing (d) printed multilayer preforms before curing and (e) the setup of oven curing and vacuum bagging (f) & (g) demonstration with complex geometries.

(Fig. 2c) for 3D printing of the produced filaments. Due to the low viscosity of the epoxy, a PTFE tube was inserted through the heat block to the nozzle tip, so the print-head can be protected from problems of melted epoxy. Compared with CCF/thermoplastic filaments, the adhesion of CCF/epoxy is relatively weak, as the material is not cured then. Therefore, the print bed was coated in a layer of PVA and not heated during the process for fast cooling in order to ensure the bonding between the printed filament and the bed. The printing temperature and speed were set to 90 °C and 300 mm/min, respectively. Based on the printing experience, a higher temperature could slightly improve the adhesion but more melted epoxy would accumulate at the feeding channel and thus cause nozzle clogging. The recommended range of printing temperature is between 80 °C and 100 °C for continuous printing and it should be lowered while printing the shape corners and large curvatures with a slow speed. The off-distance between the bed and nozzle tip, equal to the thickness of each printed layer, was set to 0.1 mm, thus the heated filament was pressed on the bed by the filleted nozzle tip and a width of about 1 mm was obtained for the single printed strip.

A two-stage curing with vacuum bagging was conducted for the printed composites preforms. The set-up of the oven curing is shown in Fig. 2 a & e. The temperature was firstly ramped to 120 °C for 1 h, melting the powder. And then the epoxy was cured at 180 °C for 2 h. For the relatively thin plates in this study, the vacuum pressure can be directly applied to the specimen via the bagging, and a peel ply was placed between them to absorb the significant excess of leaked epoxy and easily remove the specimen after curing. For the specimens with complex geometries, table salt was sprinkled around to better maintain the geometry (Fig. 2e), which was also adopted in Ref. [29]. After consolidation, the impregnated salt particle can be easily removed by water rinsing and genteelly polishing. Fig. 2 f & g present a spanner and a lattice-pattern paraglider structure made using the produced filaments and above manufacturing process, which demonstrated the design freedom for complex geometries.

3. Mechanical tests and results

Mechanical tests were performed using an MTS Criterion® Model 45 (C45.305) with a 300 kN load cell. A crosshead speed of 0.5 mm/min was used and the specimens were clamped in hydraulic grips with a pressure of approx. 80 bar. Due to the relatively-thin thickness, all the specimens were end tabbed with ±45° GRFP and VFTA400 adhesive film sourced from SHD Composites Ltd, which acts to minimise strain concentrations at the gripping points.

3.1. Uniaxial tensile tests of UD-0° specimen

Tensile testing of unidirectional (UD) 0° samples were carried out according to ASTM D3039 (Standard Test Method for Tensile Properties of Polymer Matrix Composite). The length, width and thickness of the samples were 200 mm, 15 mm and 1 mm, respectively. Before that, a UD 0° specimen was cut into 5 pieces, embedded in epoxy and then polished to observe the cross-section via scanning electron microscope (SEM). As shown in Fig. 3a, images of the cross-sections were observed using a

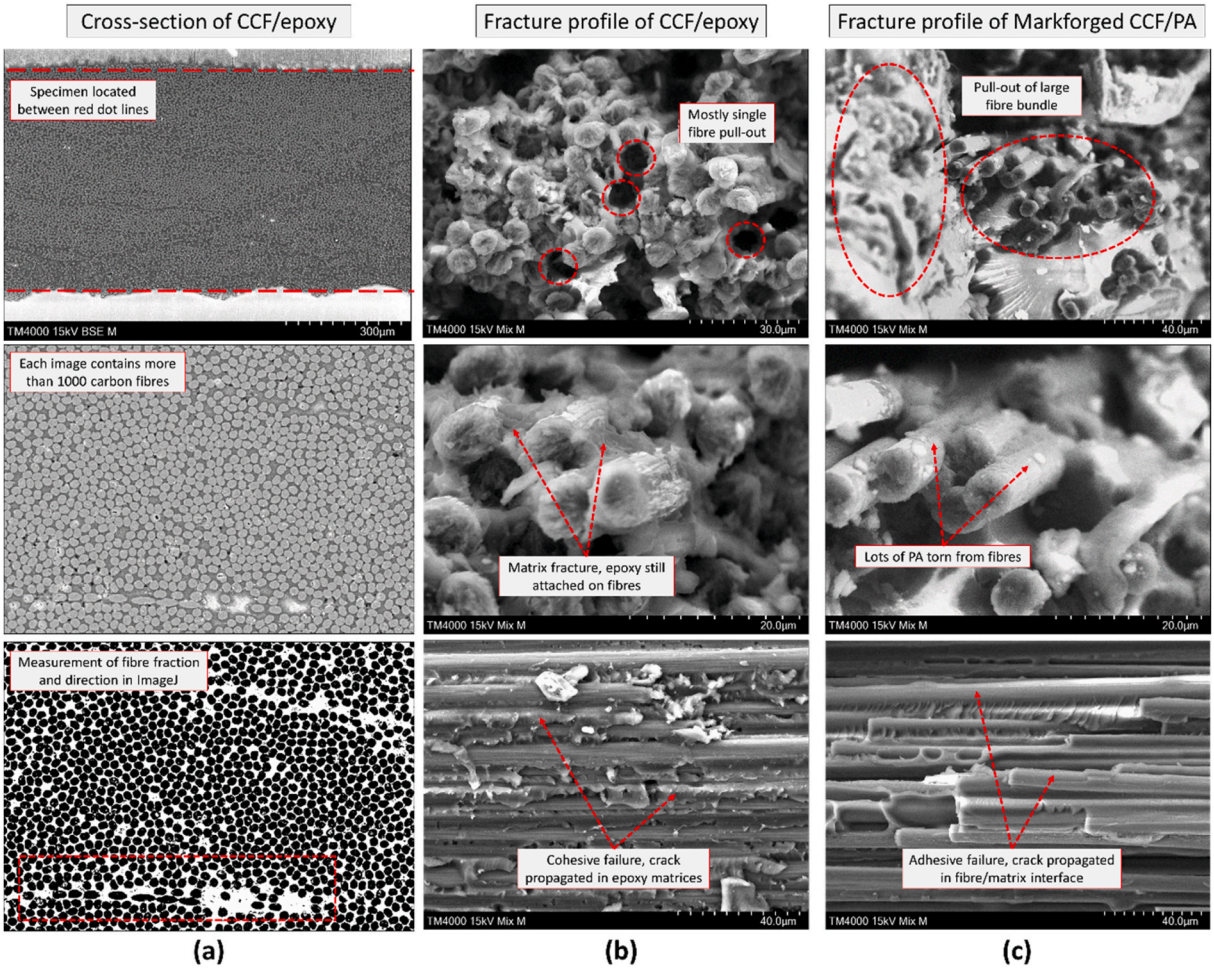

Fig. 3. SEM observation for (a) the cross-section of CCF/epoxy (b) fracture profiles of UD 0° CCF/epoxy sample and (c) fracture profiles of UD 0° Markforged® CCF/PA sample.

HITACHI® TM400 Tabletop Microscope, in which the porosity and average fibre volume fraction were measured using ImageJ software as 0.3% and 55.9%, respectively. The tensile modulus and strength in the fibre direction were 98.23 GPa and 1372.4 MPa, respectively, which is comparable with the typical aluminium/titanium alloys (see Fig. 4 a & b) [38–43]. Same mechanical tests were also conducted for the Markforged® commercial 1K CCF/PA filament (see Fig. 4c). Compared with that, the modulus and strength of produced filaments were increased by 65.6% and 67.2%, respectively. The comparison of their fracture profile in Fig. 3 b & c explains the improvement of the properties. Besides the higher fibre fraction, the CCF/epoxy sample in this study exhibited better wetting between fibre/matrix. Fig. 3b showed that matrix failure dominated in the fractured area of CCF/epoxy with shattered epoxy attached on the fibres, while lots of matrix was torn from fibres in the CCF/PA and thus the smooth surfaces of fibres became visible. Although the partition of specimens happened in both samples, cracks propagated in the CCF/epoxy matrix (cohesive failure) and conversely cracks propagated in the fibre/matrix interface in CCF/PA (adhesive failure). This respectively caused single fibre pull-out and large fibre bundle pull-out, and correspondingly led to splitting fracture mode of CCF/epoxy and step-like fracture mode of CCF/PA in the macro level [44].

However, a drop in mechanical properties was found compared with traditionally-manufactured composites, for example, the tensile modulus and strength were lower than those of hand-laid up and tensioned composites using the same powder epoxy as the matrix [37], by 27% and 44%, respectively. Therefore, the direction parameter f of printed composites was measured using ImageJ to analyse the degree of fibre straightness [45]:

$$f = \frac{\sum_{i=1}^{n} (D_{i,min}/D_{i,max})}{n}$$

where n is the number of carbon fibre, $D_{i,min}$ and $D_{i,max}$ are the minimum and maximum diameter and f indicates how far a fibre deviates from a perfect circle. A total of 50 images were analysed and each image contains more than 1000 carbon fibres as in Fig. 3a. More than 50000 fibres were analysed and the direction parameter f of printed composites was measured as 0.79. Compared to the hand-laid up and tensioned composites with $f = 0.95$ [46], the analysis indicated that fibre misalignment was one of the reasons for the drop of tensile modulus, which was contributed by the printing and curing process as discovered in our previous studies [12,46]. As for the tensile strength, the fibre breakage caused in the printing process is assumed to be one of the reasons [12], and more importantly, the strength difference between T300 and T700 carbon fibre resulted in the drop, i.e. 3530 MPa vs 4900 MPa [47,48]. The 1K carbon fibre tow used in the current printing experiments was T300, which was the only 1K carbon fibre tow available on the market, whilst 24K T700 was used in previous hand-laid up composites using the same epoxy [37]. Although competitive fibre fraction and porosity can be achieved in this study for 3D printing, some manufactured defects,

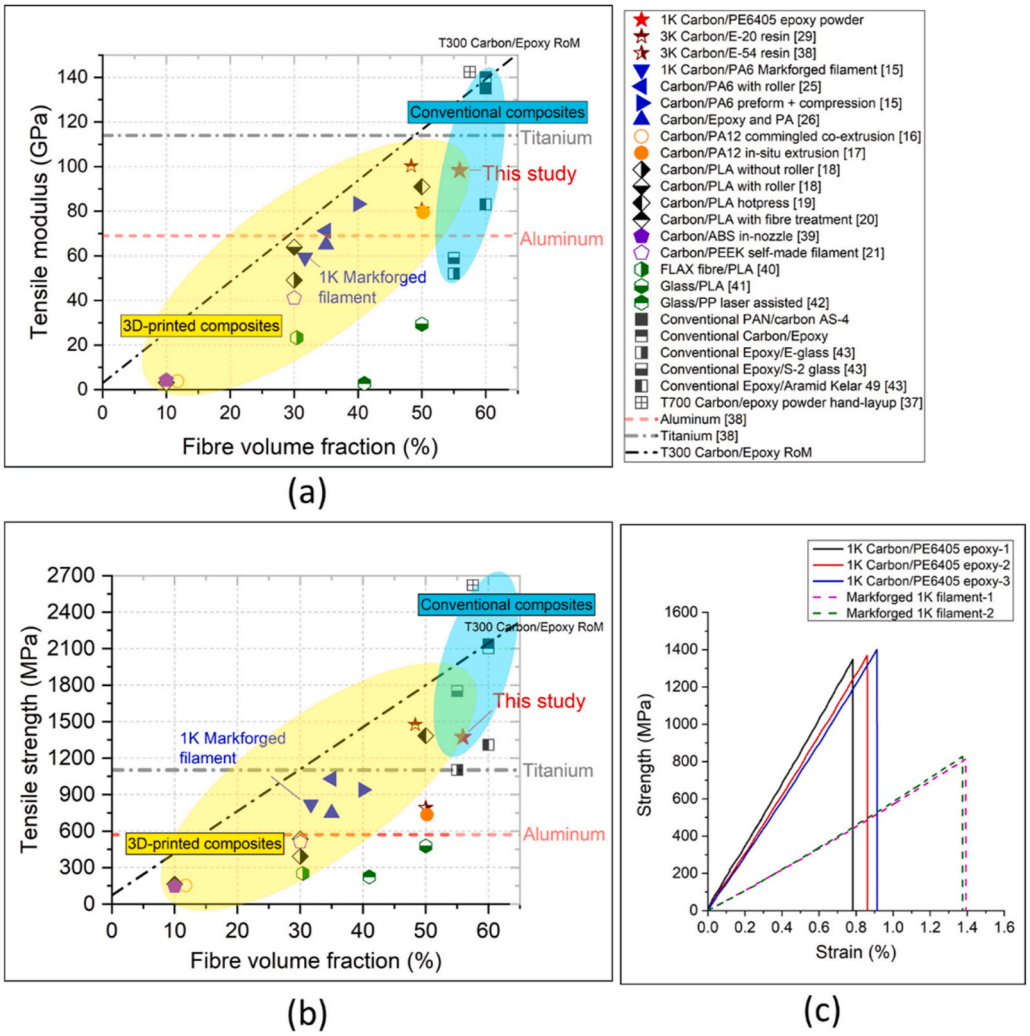

Fig. 4. Comparison chart of 3D printed continuous fibre reinforced composites: (a) tensile modulus and fibre volume fraction; (b) tensile strength and fibre volume fraction; and (c) stress-strain of UD 0° specimens.

such as fibre misalignment and breakage still exist. Therefore, the strategy for the development of additive manufacturing is to fabricate composites with complex geometries and customised fibre paths, based on the advantages of the small fibre tow and the freedom for design and manufacturing. Therefore, it would be less useful to compare 3D-printed composites with traditionally manufactured composites without considering the design of anisotropic properties [11], and the following section will illustrate the cCFRP composites with tailored fibre paths.

3.2. Open-hole tension tests of specimens with tailored fibre paths

Uniaxial tensile testing of open-hole plates was conducted as another case study as per ASTM D5766 (Standard Test Method for Open-Hole Tensile Strength of Polymer Matrix Composite Laminates), in which the width to diameter ratio was set to 2. The 'drilled' samples were manufactured via extrusion-based printing and then mechanically drilled using an ERBAUER® step drill bit, with about 1500 mm/min feed rate and 600 rpm cutting speed. The results of 'drilled' samples from the CCF/Epoxy and CCF/PA filaments are used for comparison. For the 'stress-lines' samples, the principal stress trajectories were generated from finite element analysis (FEA) of a neat polymer matrix based on the tensile loading condition and used as the guidance for the path design of continuous carbon fibres [13,49]. Continuous fibres were placed along with maximum and minimum stress trajectories alternately layer by layer. The printing of stress-lines fibre paths demonstrates the design freedom of 3D printing for the produced CCF/epoxy filament, as well as the potential to achieve better mechanical performance. It should be noted that more layers were printed for 'stress-lines' samples. In order to better compare their mechanical performance, the thicknesses of the samples were measured after curing for the calculations of strength and stiffness.

As shown in Fig. 5a, the ultimate tensile stress of the 'stress-lines' sample was improved by 90%–95%, compared with the 'drilled' sample. The stiffness in the longitudinal direction, however, was decreased due to half of the layers/fibres being printed along the minimum principal stress trajectories. The failure mode of the CCF/epoxy 'drilled' specimen is typically brittle LGM (lateral, gauge and middle) as described in the ASTM standard, in which the tensile failure laterally crossed the centre of the hole with splits. And the CCF/PA 'drilled' specimen experienced partition in the longitudinal direction, as mentioned before, due to the weak fibre/matrix interface. On the contrary, the 'stress-lines' specimen exhibits a rare fracture pattern with several irregular cracks initiating from the edge of the hole.

The digital image correlation (DIC) measurement of maximum principal strain in Fig. 5b explains how the fibre paths re-distribute the stress. Among them, CCF/epoxy and CCF/PA 'drilled' specimen exhibited the same concentration at the left and right peripheries of the hole during their elastic stage, but the stress-lines transferred the load to the whole circumference of the hole and showed an even distribution. Prior to the failure of the CCF/epoxy 'drilled' sample (same speed of cross-head, +66s from the beginning of loading), the strain concentration is located at the immediate left and right edges of the hole and extends along the longitudinal direction, but the strain of 'stress-lines' distributes evenly with only 62% of the maximum value of CCF/epoxy 'drilled' at that time. Prior to the failure of 'stress-lines', the high-value strain distributes evenly around the hole, along with a maximum value that is 41% higher than that of CCF/epoxy 'drilled', which indicated the concentrated stress was dispersed around the hole and more faraway continuous fibres participle in the load-carrying.

4. Conclusions

This study presents a filament fabrication tapeline to produce environment-friendly and low-cost 1K continuous carbon fibre filaments for material-extrusion based 3D printing. The thermoset powder-based epoxy is electrostatically deposited on the dry carbon fibre tow and heated by infrared lighting. Due to the low viscosity of the epoxy and the large melting/curing temperature gap, it enables separated filament fabrication and printing processes and good wettability is achieved. The produced filaments are 3D printed according to tailored fibre paths, followed by oven curing with vacuum bagging to manufacture composites with low porosity and high fibre volume fraction. The experimental study demonstrates the competitive mechanical performance and the manufacturing with complex geometries and designed fibre paths, which promises the opportunity to widen the industrial applications of 3D-printed continuous carbon fibre reinforced composites for lightweight structures. It should be noted that, similarly to other types of thermoset filaments, the CCF/epoxy filament produced from this study needs additional post-processing after the 3D printing. The printing system should be improved with the use of fast-cure epoxy in future filament fabrication, in order to reduce the fibre misalignment in the finished parts. For the powder-based epoxy tapeline, the parametric

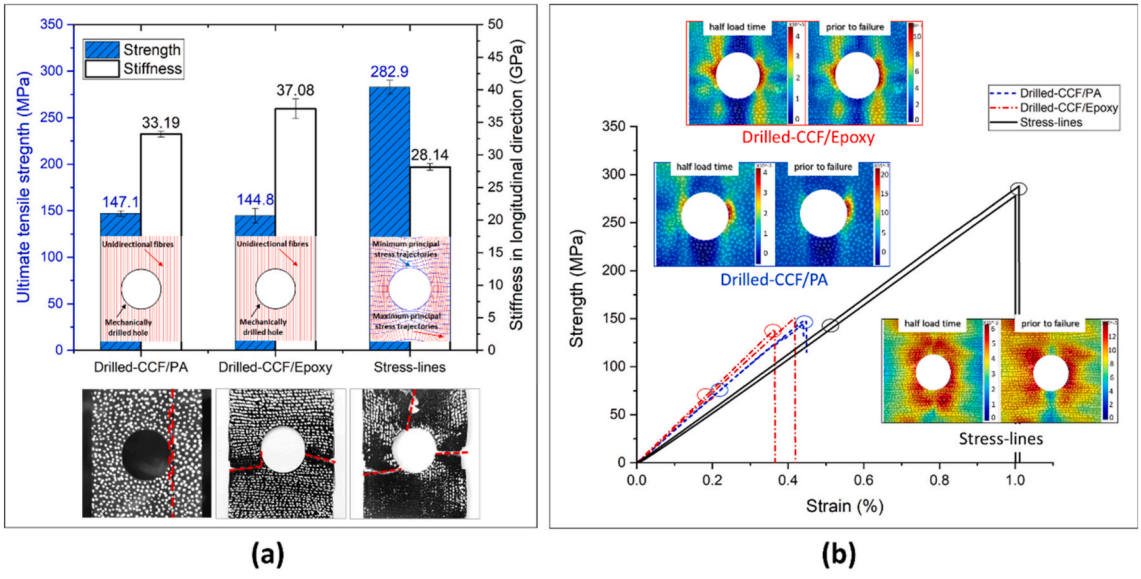

Fig. 5. (a) The mechanical performance, paths design and crack propagation of open-hole composites (b) The stress-strain curves with the DIC results measured at half load time and prior to failure.

study can be further performed to tailor the material fraction, fibre number and fibre type in the filament.

CRediT authorship contribution statement

Haoqi Zhang: Methodology, Writing – original draft, Visualization, Data curation. **Ka Zhang:** Methodology, Writing – original draft, Visualization, Data curation. **Aonan Li:** Methodology, Writing – original draft, Visualization, Data curation. **Lei Wan:** Methodology, Writing – original draft, Visualization, Data curation. **Colin Robert:** Methodology, Writing – review & editing. **Conchúr M. Ó Brádaigh:** Methodology, Writing – review & editing. **Dongmin Yang:** Conceptualization, Investigation, Writing – review & editing, Project administration, Supervision.

Declaration of competing interest

The authors declare that they have no known competing financial interests or personal relationships that could have appeared to influence the work reported in this paper.

Data availability

Data will be made available on request.

References

[1] B. Brenken, E. Barocio, A. Favaloro, V. Kunc, R.B. Pipes, Fused filament fabrication of fiber-reinforced polymers: a review, Addit. Manuf. 21 (2018) 1–16.
[2] X. Wang, M. Jiang, Z. Zhou, J. Gou, D. Hui, 3D printing of polymer matrix composites: a review and prospective, Compos. B Eng. 110 (2017) 442–458.
[3] J. Frketic, T. Dickens, S. Ramakrishnan, Automated manufacturing and processing of fiber-reinforced polymer (FRP) composites: an additive review of contemporary and modern techniques for advanced materials manufacturing, Addit. Manuf. 14 (2017) 69–86.
[4] G. Liu, Y. Xiong, L. Zhou, Additive manufacturing of continuous fiber reinforced polymer composites: design opportunities and novel applications, Compos. Commun. (2021) 27.
[5] F. Ning, W. Cong, Z. Hu, K. Huang, Additive manufacturing of thermoplastic matrix composites using fused deposition modeling: a comparison of two reinforcements, J. Compos. Mater. (2017) 3733–3742.
[6] D. Yang, H. Zhang, J. Wu, E.D. McCarthy, Fibre Flow and Void Formation in 3D Printing of Short-Fibre Reinforced Thermoplastic Composites: an Experimental Benchmark Exercise, Additive Manufacturing, 2020.
[7] C.D. Armstrong, N. Todd, A.T. Alsharhan, D.I. Bigio, R.D. Sochol, A 3D printed morphing nozzle to control fiber orientation during composite additive manufacturing, Adv. Mater. Technol. 6 (1) (2020).
[8] D. Kokkinis, M. Schaffner, A.R. Studart, Multimaterial magnetically assisted 3D printing of composite materials, Nat. Commun. 6 (2015) 8643.
[9] Y. Kanarska, E.B. Duoss, J.P. Lewicki, J.N. Rodriguez, A. Wu, Fiber motion in highly confined flows of carbon fiber and non-Newtonian polymer, J. Non-Newtonian Fluid Mech. 265 (2019) 41–52.
[10] S.M.F. Kabir, K. Mathur, A.-F.M. Seyam, A Critical Review on 3D Printed Continuous Fiber-Reinforced Composites: History, Mechanism, Materials and Properties, Composite Structures, 2020, p. 232.
[11] P. Zhuo, S. Li, I.A. Ashcroft, A.I. Jones, Material extrusion additive manufacturing of continuous fibre reinforced polymer matrix composites: a review and outlook, Compos. B Eng. (2021).
[12] H. Zhang, J. Chen, D. Yang, Fibre misalignment and breakage in 3D printing of continuous carbon fibre reinforced thermoplastic composites, Addit. Manuf. 38 (2021).
[13] H. Zhang, D. Yang, Y. Sheng, Performance-driven 3D printing of continuous curved carbon fibre reinforced polymer composites: a preliminary numerical study, Compos. B Eng. 151 (2018) 256–264.
[14] H. Zhang, A.N. Dickson, Y. Sheng, T. McGrail, D.P. Dowling, C. Wang, et al., Failure analysis of 3D printed woven composite plates with holes under tensile and shear loading, Compos. B Eng. (2020) 186.
[15] Q. He, H. Wang, K. Fu, L. Ye, 3D printed continuous CF/PA6 composites: effect of microscopic voids on mechanical performance, Compos. Sci. Technol. (2020) 191.
[16] M. Reis Silva, A.M. Pereira, N. Alves, G. Mateus, A. Mateus, C. Malça, Development of an additive manufacturing system for the deposition of thermoplastics impregnated with carbon fibers, J. Manuf. Mater. Proc. 3 (2) (2019) 35.
[17] T. Liu, X. Tian, Y. Zhang, Y. Cao, D. Li, High-pressure interfacial impregnation by micro-screw in-situ extrusion for 3D printed continuous carbon fiber reinforced nylon composites, Compos. Appl. Sci. Manuf. (2020) 130.
[18] R. Omuro, M. Ueda, R. Matsuzaki, A. Todoroki, Y. Hirano, Three-dimensional Printing of Continuous Carbon Fiber Reinforced Thermoplastics by In-Nozzle Impregnation with Compaction Roller. 21st International Conference on Composite Materials, 2017, pp. 20–25. Xian, China.
[19] M. Yamawaki, Y. Kouno, Fabrication and mechanical characterization of continuous carbon fiber-reinforced thermoplastic using a preform by three-dimensional printing and via hot-press molding, Adv. Compos. Mater. (2017) 1–11.
[20] J. Qiao, Y. Li, L. Li, Ultrasound-assisted 3D printing of continuous fiber-reinforced thermoplastic (FRTP) composites, Addit. Manuf. 30 (2019).
[21] Y. Chen, Z. Shan, X. Yang, Y. Song, A. Zou, Preparation of CCF/PEEK filaments together with property evaluation for additive manufacturing, Compos. Struct. (2021).
[22] M. Luo, X. Tian, J. Shang, W. Zhu, D. Li, Y. Qin, Impregnation and interlayer bonding behaviours of 3D-printed continuous carbon-fiber-reinforced poly-ether-ether-ketone composites, Compos. Appl. Sci. Manuf. 121 (2019) 130–138.
[23] G. Struzziero, M. Barbezat, A.A. Skordos, Consolidation of continuous fibre reinforced composites in additive processes: a review, Addit. Manuf. 48 (2021).
[24] G.T. Mark, A.S. Gozdz, Methods for Composite Filament Fabrication in Three Dimensional Printing, U.S. Patent, 2015.
[25] M. Ueda, S. Kishimoto, M. Yamawaki, R. Matsuzaki, A. Todoroki, Y. Hirano, et al., 3D compaction printing of a continuous carbon fiber reinforced thermoplastic, Compos. Appl. Sci. Manuf. (2020) 137.
[26] A. Azarov, F. Antonov, V. Vasil'ev, M. Golubev, D. Krasovskii, A. Razin, et al., Development of a two-matrix composite material fabricated by 3D printing, Polym. Sci. 10 (1) (2017) 87–90.
[27] M. Invernizzi, G. Natale, M. Levi, S. Turri, G. Griffini, UV-assisted 3D printing of glass and carbon fiber-reinforced dual-cure polymer composites, Materials 9 (7) (2016).
[28] M.A. Rahman, M.Z. Islam, L. Gibbon, C.A. Ulven, J.J. La Scala, 3D printing of continuous carbon fiber reinforced thermoset composites using UV curable resin, Polym. Compos. 42 (11) (2021) 5859–5868.
[29] Y. Ming, Y. Duan, B. Wang, H. Xiao, X. Zhang, A novel route to fabricate high-performance 3D printed continuous fiber-reinforced thermosetting polymer composites, Materials 12 (9) (2019).
[30] Misev Tv, Vd Linde, Powder coatings technology: new developments at the turn of the century, Prog. Org. Coating 34 (1–4) (1998) 160–168.
[31] V. Jagadeeswari, A. Sahoo, An overview on dry powder coating in advancement to electrostatic dry powder coating used in pharmaceutical industry, Powder Technol. (2022), 117214.
[32] N. Ayrilmis, A review on electrostatic powder coatings for the furniture industry, Int. J. Adhesion Adhes. 113 (2022), 103062.
[33] A. Thomas, K. Saleh, P. Guigon, C. Czechowski, Characterisation of electrostatic properties of powder coatings in relation with their industrial application, Powder Technol. 190 (1–2) (2009) 230–235.
[34] J.M. Maguire, K. Nayak, C.M. Ó Brádaigh, Characterisation of epoxy powders for processing thick-section composite structures, Mater. Des. 139 (2018) 112–121.
[35] J.M. Maguire, K. Nayak, C.M.Ó. Brádaigh, Characterisation of epoxy powders for processing thick-section composite structures, Mater. Des. 139 (2018) 112–121.
[36] D. Mamalis, T. Flanagan, C.M.Ó. Brádaigh, Effect of fibre straightness and sizing in carbon fibre reinforced powder epoxy composites, Compos. Appl. Sci. Manuf. 110 (2018) 93–105.
[37] C. Robert, T. Pecur, J.M. Maguire, A.D. Lafferty, E.D. McCarthy, C.M. Ó Brádaigh, A novel powder-epoxy towpregging line for wind and tidal turbine blades, Compos. B Eng. (2020) 203.
[38] W. Hao, Y. Liu, H. Zhou, H. Chen, D. Fang, Preparation and characterization of 3D printed continuous carbon fiber reinforced thermosetting composites, Polym. Test. 65 (2018) 29–34.
[39] C. Yang, X. Tian, T. Liu, Y. Cao, D. Li, 3D printing for continuous fiber reinforced thermoplastic composites: mechanism and performance, Rapid Prototyp. J. (2017).
[40] A. Le Duigou, A. Barbé, E. Guillou, M. Castro, 3D printing of continuous flax fibre reinforced biocomposites for structural applications, Mater. Des. 180 (2019), 107884.
[41] B. Akhoundi, A.H. Behravesh, A. Bagheri Saed, Improving mechanical properties of continuous fiber-reinforced thermoplastic composites produced by FDM 3D printer, J. Reinforced Plast. Compos. Adv. Mater. 38 (3) (2019) 99–116.
[42] P. Parandoush, L. Tucker, C. Zhou, D. Lin, Laser assisted additive manufacturing of continuous fiber reinforced thermoplastic composites, Mater. Des. 131 (2017) 186–195.
[43] D. Chung, Carbon Fiber Composites, Elsevier, 2012.
[44] Y. Ma, Y. Yang, T. Sugahara, H. Hamada, A study on the failure behavior and mechanical properties of unidirectional fiber reinforced thermosetting and thermoplastic composites, Compos. B Eng. 99 (2016) 162–172.
[45] M. Çelik, T. Noble, F. Jorge, R. Jian, C.M. Ó Brádaigh, C. Robert, Influence of line processing parameters on properties of carbon fibre epoxy towpreg, J. Compos. Sci. 6 (3) (2022).
[46] D. Mamalis, T. Flanagan, C.M. Ó Brádaigh, Effect of fibre straightness and sizing in carbon fibre reinforced powder epoxy composites, Compos. Appl. Sci. Manuf. 110 (2018) 93–105.
[47] T. Industries, T300-Technical-Data-Sheet. https://www.toraycma.com/wp-content/uploads/T300-Technical-Data-Sheet-1.pdf.pdf, 2018. (Accessed 11 April 2022).
[48] T. Industries, T700-Technical-Data-Sheet. https://www.toraycma.com/wp-content/uploads/T700S-Technical-Data-Sheet-1.pdf.pdf, 2018. (Accessed 11 April 2022).
[49] H. Zhang, A. Li, J. Wu, B. Sun, C. Wang, D. Yang, Effectiveness of fibre placement in 3D printed open-hole composites under uniaxial tension, Compos. Sci. Technol. (2022), 109269.